AIP | Applied Physics Letters

Millimeter scale electrostatic mirror with sub-wavelength holes for terahertz wave scanninga)

Hyeon-Cheol Park, Jung-Hwan Lee, Sang-Gil Park, Dae-Su Yee, and Ki-Hun Jeong

Citation: Applied Physics Letters **102**, 031111 (2013); doi: 10.1063/1.4788915
View online: http://dx.doi.org/10.1063/1.4788915
View Table of Contents: http://scitation.aip.org/content/aip/journal/apl/102/3?ver=pdfcov
Published by the AIP Publishing

Millimeter scale electrostatic mirror with sub-wavelength holes for terahertz wave scanning[a)]

Hyeon-Cheol Park,[1,b)] Jung-Hwan Lee,[1,b)] Sang-Gil Park,[1] Dae-Su Yee,[2] and Ki-Hun Jeong[1,c)]
[1]*Department of Bio and Brain Engineering, Korea Advanced Institute of Science and Technology (KAIST), 291 Daehak-ro, Yuseong-gu, Daejeon 305-701, South Korea*
[2]*Center for Safety Measurement Korea Research Institute of Standards and Science (KRISS), 267 Gajeong-ro, Yuseong-gu, Daejeon 305-340, South Korea*

(Received 16 October 2012; accepted 1 January 2013; published online 24 January 2013)

This work reports the design, microfabrication, and characterization of highly reflective electrostatic mirrors with sub-wavelength holes for scanning terahertz (THz) waves. The mirror consists of an aluminum coated silicon mirror plate precisely assembled on the top of two axis torsional microactuators. The mirror plate with sub-wavelength microholes not only provides high reflectivity over 98% at THz waves by decoupling the surface plasmon resonance but also reduces air damping by allowing air to flow through the mirror plate during the mirror scanning. The device can provide many opportunities for miniaturized THz time domain spectroscopic imaging systems. © *2013 American Institute of Physics*. [http://dx.doi.org/10.1063/1.4788915]

Electromagnetic radiation at terahertz (THz) frequencies offers excellent penetration for most nonpolar and nonmetallic materials such as clothes, polymer, glass, ceramics, or semiconductors.[1–3] For biochemical molecules, terahertz time domain spectroscopy (THz TDS) enables label-free detections of diverse vibration modes depending on collective molecular oscillations or unfolding, which can identify non-invasive and label-free biological fingerprints such as deoxyribonucleic acid (DNA) hybridization,[4] protein conformation,[5] or early cancer detections.[6,7] An extension of this technique is THz spectroscopic imaging, where a series of measurements can be compiled into the two-dimensional (2D) spatial representation. THz imaging with transmission or reflection type has been recently demonstrated by scanning a target sample and then determining the spatial distribution of epithermal cancer signature.[6,7] However, conventional THz imaging systems comprising THz emitters, detectors, and scanning units are large in size and limited in *ex-vivo* experiment of excised tissues or organs. Moreover, the systems have been restricted to particular biomedical applications due to small penetration depth of THz waves in tissues caused by high water absorption.[8] This physical limitation stimulates the miniaturization of THz imaging systems for diverse biomedical applications. More recently, THz based endoscopes have been reported by miniaturizing some constituents of THz TDS systems such as source and detector.[9] However, the previous work still performs single point detection within a limited field-of-view due to the lack of a scanning unit, which is a crucial component for THz TDS imaging systems. Recently, micro-electro-mechanical-systems (MEMS) enables the miniaturization of optical scanning units for functional microendoscopic applications such as optical coherence tomography,[10–12] confocal,[13] or multi-photon imaging.[14] In particular, scanning MEMS mirrors offer many advantages of large scanning angles with low power consumption and low voltage operation. However, scanning MEMS mirrors for THz TDS still have some significant technical challenges in implementing the mirror size large enough than THz wavelengths (typically 30 μm to 3 mm in wavelength for 0.1–10 THz). For example, millimeter-scale scanning MEMS mirrors suffer from high air damping and high inertia with low fill-factor.

This work reports the design, microfabrication, and characterization of highly reflective MEMS mirrors with sub-wavelength holes for scanning THz waves. Fig. 1(a) illustrates a THz scanning MEMS mirror, which consists of an aluminum coated silicon mirror plate with millimeter scale precisely assembled on the top of two axis torsional microactuators with electrostatic actuation. The mirror plate and torsional microactuators were separately fabricated and then vertically assembled to ensure compact packaging. Besides, sub-wavelength microhole arrays were implemented on a mirror surface to reduce air damping by allowing air to flow through the mirror plate without sacrifice of reflectivity at THz frequencies. Fig. 1(b) shows an optical image of a fully assembled THz beam scanning MEMS mirror where

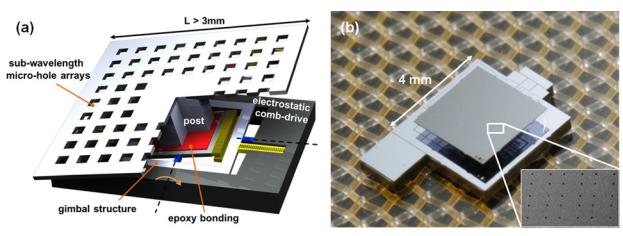

FIG. 1. Millimeter scale MEMS mirror with subwavelength microhole arrays for THz wave scanning: (a) a schematic diagram of millimeter-scale scanning MEMS mirror with sub-wavelength microhole arrays and (b) an optical image of the fully integrated MEMS mirror and a SEM image of microhole arrays on the aluminum coated silicon mirror plate (inset). A silicon mirror plate with microhole arrays is vertically assembled with two axis torsional microactuators.

[a)]Millimeter-Scale Scanning MEMS Mirror with Sub-Wavelength Microhole Arrays for Terahertz Wave Scanning, published as part of the IEEE Optical MEMS and Nanophotonics 2012, Banff, Canada, August 2012.
[b)]H.-C. Park and J.-H. Lee contributed equally to this work.
[c)]Electronic mail: kjeong@kaist.ac.kr.

the inset image indicates the scanning electron microscopic image of sub-wavelength microhole arrays on the mirror plate (microhole diameter less than $\lambda/30$ at 1 THz).

The design of the scanning MEMS mirror was done by taking both optical and mechanical requirements of scanning resolution, THz wave reflectivity, and imaging speed. In particular, the number of resolvable spots of a THz scanning mirror, termed a scanning resolution N, is determined by $\theta_m D/\lambda$, where θ_m is the total optical scanning angle, D is the mirror size, and λ is the wavelength of a THz wave.[15] For conventional THz TDS imaging systems, the maximum detection speed is limited below 1 kHz, which allows 10 frames per second in Raster scanning for 10×10 pixels. In this case, the spot number corresponds to below $N = 5$ based on Nyquist criterion. For this particular design, the mirror plate is 3 mm $\times$ 3 mm in size for conventional maximum optical scanning angle of 1/2 radians and the resonant frequency of MEMS mirror was initially designed to operate at 100 Hz.

During the mirror scan, the air damping force proportionally increases with the square of mirror size whereas the scanning amplitude decreases. The damping force can be effectively reduced by implementing sub-wavelength microholes on the mirror plate that allows air to pass through the plate and substantially decreases the air damping pressure beneath the plate. The damping force of a thin perforated plate is inversely proportional to the ratio, η, between the microhole size, r_i, and the hole period, r_c.[16] The increase of microhole size at constant period decreases the damping constant relatively much faster than the mirror inertia. For example, the damping constant is reduced by about 60% for the ratio of only 0.1 whereas the inertia remains about 99%. However, the ratio of microholes is limited by THz wave reflectivity of the aluminum coated mirror plate. The microholes at sub-wavelength scale can reduce the diffraction loss of THz waves nevertheless they can also cause extraordinary light transmission or coupling loss by the surface plasmon resonance on metal-dielectric interface, which results in the significant reduction of THz reflectivity.[17–20] In order to avoid coupling of THz waves with surface plasmons on the mirror surface and also to secure high reflectivity of THz waves, the physical dimension of rectangular sub-wavelength microhole arrays was determined using a finite-difference time-domain (FDTD) analysis. Fig. 2(a) describes a numerical model of rectangular and sub-wavelength microholes perforated on a 40 μm thick silicon substrate coated with a 1 μm thick aluminum layer. In this calculation, the refractive index of silicon was 3.4 and the aluminum layer was approximated as a perfect electric conductor to reduce the computational load. The periodic boundary condition was used for embodying sub-wavelength microhole arrays. These approximations are valid on THz frequency region.[21] The physical dimension of rectangular microholes was then altered from 10 μm to 80 μm in width and from 60 μm to 200 μm in period. Fig. 2(b) demonstrates THz (0.1–2 THz) wave reflectivities on the mirror surface with different microhole widths at a constant period of 100 μm. Dips in specular reflectivity are observed due to the surface plasmon resonance on the aluminum-silicon interface. When the microhole widths were larger than 10 μm, the transmission dips were observed at 0.93 THz for [$\pm$1, 0] modes and at 1.3 THz for [$\pm$1, $\pm$1] modes, which correspond to the analytical approximation.[18] The surface plasmon mode also depends on the dielectric constant of substrate. The reduction in effective index of the substrate as increasing the microhole width results in a blue-shift of transmission dip. However, the dips were not observed below the width of 10 μm, which shows high reflectivity over 99% of broadband THz waves. Besides, the microhole width of 10 μm was also valid for different periods as shown in Fig. 2(c). Therefore, the size of microholes was set to be 10 μm and some irregularities of a period were also implemented to avoid unexpected surface plasmon resonance effect.

THz wave scanning MEMS mirrors were fabricated by standard silicon-on-insulator (SOI) process and out-of-plane microassembly techniques. The mirror plate and MEMS microactuator were separately fabricated at the wafer level and vertically assembled at chip level as shown in Fig. 3. First, the microfabrication of mirror plates is described in Fig. 3(a). 1 μm thick silicon oxide (SiO_2) was deposited on the back side of a 6 in. SOI wafer (top Si 40 μm, buried oxide (BOX) 2 μm, and bottom Si 500 μm in thickness) using plasma enhanced chemical vapor deposition (PECVD). The mirror plates with perforating microholes were defined on the top silicon by the first deep reactive ion etching (DRIE) process with a predefined photoresist (PR) mask. The footstep of mirror holder with 50 μm in height was fabricated on the bottom silicon by the second DRIE process with a composite mask of a PR and PECVD SiO_2. During the second DRIE process, two step heights of the bottom silicon were formed by etching the bottom silicon with SiO_2 mask after the PR removal. A thin aluminum layer of 200 nm in thickness, which

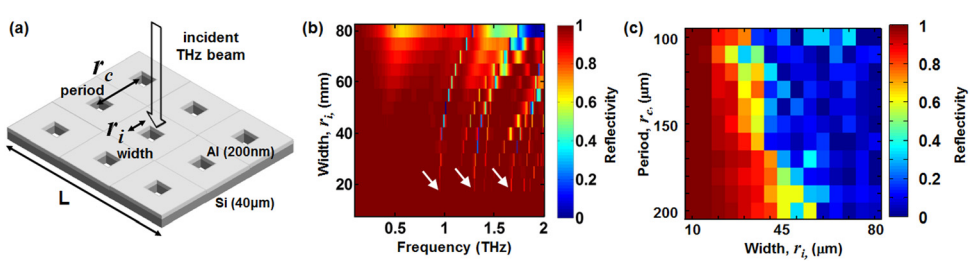

FIG. 2. THz reflectivity of aluminum coated Si mirror plates with microholes. (a) A numerical model for FDTD simulation. Rectangular and sub-wavelength microhole arrays of width r_i and period r_c were implemented on an aluminum coated silicon mirror plate. (b) Spectral THz reflectivity at a constant period of 100 μm. Dips in specular reflectivity are observed due to either extraordinary light transmission or coupling by surface plasmon resonance on the Al-Si interface. (c) THz reflectivity for different widths and periods of microholes. The microhole width below 10 μm at different periods shows high reflectivity over 99% without the dips in reflectivity.

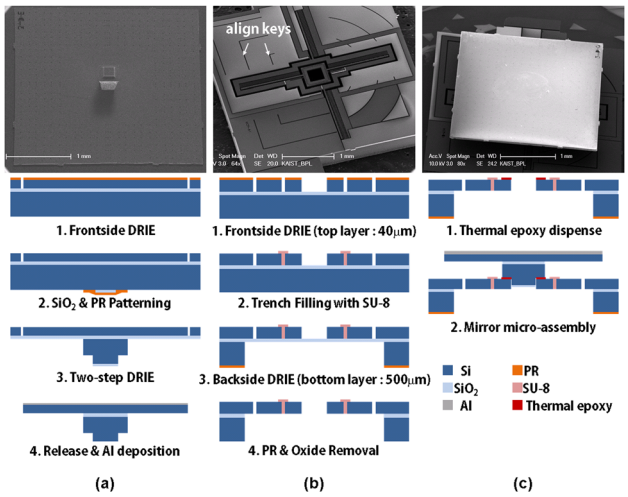

FIG. 3. Microfabrication procedures and microassembly for THz scanning MEMS mirror, which consist of (a) aluminum coated silicon mirror plate with microhole arrays, (b) two axis torsional microactuators, and (c) microassembly for mounting MEMS mirror plate on the microactuator. Both the silicon mirror plate and the microactuator are precisely assembled with thermal epoxies while monitoring pre-defined align keys on an actuator and vertical positions with top and side view microscopic cameras.

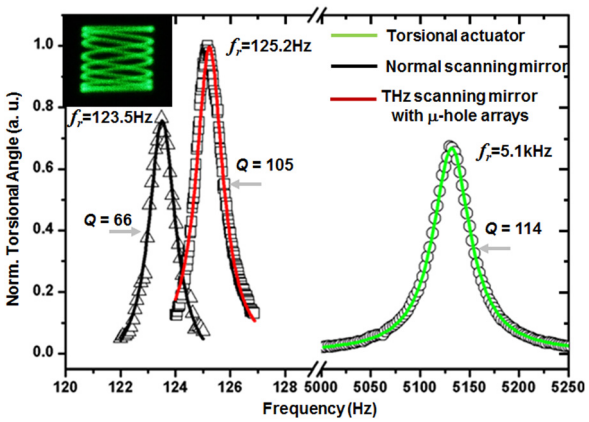

FIG. 4. Dynamic responses and optical scanning patterns of THz scanning MEMS mirror with microhole arrays; resonant frequency of a torsional actuator was 5.1 kHz with mechanical Q-factor of 114. The resonant frequency shifts to 123.5 Hz and Q-factor was decreased to 66 after mounting 3×3 mm^2 mirror plate. However, the Q-factor was increased to 105 when implementing microhole arrays on a mirror plate by minimizing the damping loss, while the resonant frequency was slightly increased due to the inertia of microholes. Two-dimensional optical scanning of the MEMS mirror was visualized using HeNe laser of 530 nm wavelength (inset).

is above twice skin depth (roughly 82 nm at 1 THz), was thermally evaporated on the top silicon surface to ensure high reflectivity for THz waves. The mirror plates were individually tethered with silicon structures on a SOI wafer and separated from the wafer by Joule heating (supplemental material S1[26]).[22,23] Next, the MEMS microactuators were separately fabricated on a 6 in. SOI wafer (top Si 40 μm, BOX 2 μm, and bottom Si 500 μm in thickness) as illustrated in Fig. 3(b). The top silicon was defined using a DRIE process with a photoresist mask. The MEMS microactuator consists of the gimbal base frame, the outer frame, and the inner frame with a mirror holder. The individual frames are suspended with two torsional silicon hinges and orthogonally actuated by electrostatic comb drives. In particular, both mechanical connection and electrical isolation between the inner and outer electrostatic comb drives of the gimbal frames were achieved with patterning SU-8 microstructures over 4 μm wide trenches. The bottom silicon was etched with DRIE and the devices were released by etching BOX with vapor phase hydrogen fluoride (HF).[24] The MEMS actuators were also tethered with silicon structures on a SOI wafer and individually separated from the wafer by Joule heating. Finally, a mirror plate and a MEMS actuator were micro-assembled by a simple two-step process. A thermal epoxy was precisely dispensed on the mirror holder of MEMS actuator using a glass micropipette with a micromanipulator (supplemental material S2[26]). The precise alignment between the silicon post of mirror plate and the mirror holder of MEMS actuator was conducted by monitoring pre-defined align keys on an actuator (indicated in Fig. 3(b)) and vertical positions with top and side view microscopic cameras (supplemental material S3[26]). The initial tolerance between the silicon pedestal of mirror post and the mirror holder of MEMS actuator was set to be 20 μm. The device was finally glued on a hotplate for 1 h at 150 °C.

The dynamic responses of scanning MEMS mirror with microhole arrays substantially vary with both inertia of silicon mirror plate and microhole arrays. The resonance frequencies of scanning MEMS mirrors were measured with a laser Doppler vibrometer. Fig. 4 shows the change in resonance frequency before and after mounting a silicon mirror plate on the MEMS actuator. The initial resonant frequency of the MEMS actuator was 5.1 kHz with a mechanical quality factor (Q-factor) of 114. After mounting a mirror plate, which has a physical dimension of 3×3 mm^2 with 40 μm in thickness, high inertia of the mirror plate shifts the resonance frequency to 123.5 Hz. Besides, the high damping force also decreases the Q-factor to 66. However, the sub-wavelength microhole arrays of 10 μm size effectively reduce the air damping force and increase the Q-factor to 105 whereas the resonant frequency shifts only about 1.4% higher due to the inertia reduction by the microholes. The high Q-factor enables a low voltage operation of DC 5 V and AC 10 V for optical scanning angles of 20°, whereas the MEMS actuator was operated at DC 20 V and AC 15 V for 7.3°. Fig. 4 inset image shows the 2D optical scanning pattern of the MEMS mirror. Helium-neon (HeNe) laser of 530 nm in wavelength was coupled with MEMS mirror to visualize the optical scanning.

THz wave scanning of the MEMS mirror was demonstrated with reflection-type THz wave measurement as illustrated in Fig. 5(a). Especially, we used an electronically controlled optical sampling (ECOPS) method for THz wave measurement, which enables us to acquire THz waveforms consecutively at 1 kHz (supplemental material S4[26]).[25] A THz pulse reflected from the MEMS mirror has a peak amplitude above 98% of that of a THz pulse reflected from a normal mirror, as shown in Fig. 5(b). THz wave scanning was finally demonstrated with the MEMS mirror. Fig. 5(c) shows that a detected THz amplitude changes with the scanning angle of the MEMS mirror. In this measurement, the MEMS mirror was scanned at 118 Hz and the THz amplitude oscillated at double the scanning frequency since the THz amplitude varies from the maximum to the minimum with the scanning angle varied from zero to the maximum during a quarter mirror scanning cycle.

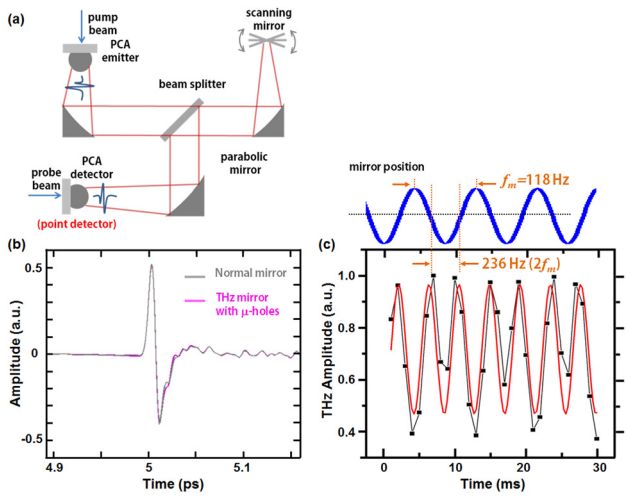

FIG. 5. Experimental demonstration of THz wave scanning using a millimeter scale scanning MEMS mirror with microhole arrays; (a) experimental set-up for reflection type THz TDS system. (b) Time-domain waveform of the reflected THz wave were well remained. (c) Change in the amplitude of 1 THz waves while the MEMS mirror scans with a scanning frequency at 118 Hz. The scanning frequency of THz waves is doubled.

In summary, a millimeter scale scanning MEMS mirror for THz wave scanning has been demonstrated using a SOI based DRIE process and microassembly techniques. The vertical assembly enables a compact packaging with large aperture. Besides, sub-wavelength microhole arrays on the mirror plate provide both high reflectivity over 98% at THz waves and low air damping during the mirror scanning. This device can provide many opportunities for miniaturizing THz TDS based imaging systems such as a hand held probes or even endoscopic catheters for advanced biomedical imaging.

This work was financially supported by the Ministry of Education, Science and Technology (MEST 20120005641, 20120006653, 2012054200) and the Ministry of Knowledge Economy (MEK 10041120) of the Korea government.

[1]B. Ferguson and X.-C. Zhang, Nature Mater. **1**(1), 26 (2002).
[2]M. Tonouchi, Nat. Photonics **1**(2), 97 (2007).
[3]C. Schmuttenmaer, Chem. Rev. **104**(4), 1759 (2004).
[4]M. Brucherseifer, M. Nagel, P. Haring Bolivar, H. Kurz, A. Bosserhoff, and R. Büttner, Appl. Phys. Lett. **77**(24), 4049 (2000).
[5]K. Kawase, Y. Ogawa, Y. Watanabe, and H. Inoue, Opt. Express **11**(20), 2549 (2003).
[6]R. M. Woodward, B. E. Cole, V. P. Wallace, R. J. Pye, D. D. Arnone, E. H. Linfield, and M. Pepper, Phys. Med. Biol. **47**(21), 3853–3863 (2002).
[7]R. M. Woodward, V. P. Wallace, R. J. Pye, B. E. Cole, D. D. Arnone, E. H. Linfield, and M. Pepper, J. Invest. Dermatol. **120**(1), 72 (2003).
[8]L. Thrane, R. H. Jacobsen, P. Uhd Jepsen, and S. R. Keiding, Chem. Phys. Lett. **240**(4), 330 (1995).
[9]Y. B. Ji, E. S. Lee, S.-H. Kim, J.-H. Son, and T.-I. Jeon, Opt. Express **17**(19), 17082 (2009).
[10]W. Jung, D. T. McCormick, Y.-C. Ahn, A. Sepehr, M. Brenner, B. Wong, N. C. Tien, and Z. Chen, Opt. Lett. **32**(22), 3239 (2007).
[11]J. Sun, S. Guo, L. Wu, L. Liu, S. Choe, B. S. Sorg, and H. Xie, Opt. Express **18**(12), 12065 (2010).
[12]K. H. Kim, B. H. Park, G. N. Maguluri, T. W. Lee, F. J. Rogomentich, M. G. Bancu, B. E. Bouma, J. F. de Boer, and J. J. Bernstein, Opt. Express **15**(26), 18130 (2007).
[13]J. T. C. Liu, M. J. Mandella, N. O. Loewke, H. Haeberle, H. Ra, W. Piyawattanametha, O. Solgaard, G. S. Kino, and C. H. Contag, J. Biomed. Opt. **15**(2), 026029 (2010).
[14]W. Jung, S. Tang, D. T. McCormic, T. Xie, Y.-C. Ahn, J. Su, I. V. Tomov, T. B. Krasieva, B. J. Tromberg, and Z. Chen, Opt. Lett. **33**(12), 1324 (2008).
[15]M. Born and E. Wolf, *Principles of Optics*, 7th ed. (Cambridge University Press, 1999), p. 949.
[16]M. Bao and H. Yang, Sens. Actuators, A **136**(1), 3 (2007).
[17]M. A. Seo, H. R. Park, S. M. Koo, D. J. Park, J. H. Kang, O. K. Suwal, S. S. Choi, P. C. M. Planken, G. S. Park, N. K. Park, Q. H. Park, and D. S. Kim, Nat. Photonics **3**(3), 152 (2009).
[18]D. Qu, D. Grischkowsky, and W. Zhang, Opt. Lett. **29**(8), 896 (2004).
[19]M. Tanaka, F. Miyamaru, M. Hangyo, T. Tanaka, M. Akazawa, and E. Sano, Opt. Lett. **30**(10), 1210 (2005).
[20]J. W. Lee, M. A. Seo, J. Y. Sohn, Y. H. Ahn, D. S. Kim, S. C. Jeoung, Ch. Lienau, and Q.-H. Park, Opt. Express **13**(26), 10681 (2005).
[21]R. Singh, A. K. Azad, J. F. O'Hara, A. J. Taylor, and W. Zhang, Opt. Lett. **33**(13), 1506 (2008).
[22]Y. S. S. Chiu, K. D. J. Chang, R. W. Johnstone, and M. Parameswaran, J. Micromech. Microeng. **16**(3), 480 (2006).
[23]H.-C. Park, C. Song, and K.-H. Jeong, Opt. Express **18**(15), 16133 (2010).
[24]Y. Fukuta, H. Fujita, and H. Toshiyoshi, Jpn. J. Appl. Phys., Part 1 **42**(6A), 3690 (2003).
[25]Y. Kim and D.-S. Yee, Opt. Lett. **35**(22), 3715 (2010).
[26]See supplementary material at http://dx.doi.org/10.1063/1.4788915 for S1–S3; microassembly procedure, S4; ECOPS measurement.